JOURNAL OF OPTOELECTRONICS AND ADVANCED MATERIALS Vol. 10, No. 10, October 2008, p. 2622 - 2630

Cadmium sulphide thin films grown by CBD: the effect of thermal annealing on the structural, electrical and optical properties

H. METIN[a*], F. SAT[a], S. ERAT[b], M. ARI[c]
[a]*University of Mersin, Department of Physics, Mersin, Turkey*
[b]*Laboratory for High Performance Ceramics EMPA-Swiss Federal Laboratories for Materials Testing & Research CH-8600 Dübendorf, Switzerland*
[c]*University of Erciyes, Department of Physics, Kayseri, Turkey*

Cadmium sulphide (CdS) thin films have been grown by the chemical bath deposition (CBD) technique using cadmium sulfate and thiourea, as the Cd^{2+} and S^{2-} ion sources. The chemically deposited films are annealed in air at different temperatures to estimate the effect of the annealing on the structural, optical and electrical properties of the films. These films have been characterized by means of X-ray powder diffraction (XRD), energy dispersive X-ray analysis (EDX), scanning electron microscopy (SEM), four point probe technique and UV-Visible spectrophotometer. From the results it is seen that the electrical resistivity, activation energy and the optical energy band gap are strongly depend on the annealing temperature. The optical band gap energy decreased from 2.43 eV to 2.39 eV with increasing the temperature. The electrical resistivity shows a decrease with the temperature with a minimum of 1.79×10^{3} Ω-cm at 800 K for the annealed film at 473 K. However, the electrical resistivity shows an increase for 573 K≤ T ≤ 773 K. With increasing the annealing temperature, the activation energy of the films decreased from 0.23 eV to 0.13 eV at low temperature region, and from 0.67 eV to 0.48 eV at high temperature region. The activation energies obtained from the absorption and resistivity measurements are compared. Also, the temperature coefficients of electrical resisitivity are determined to be between -2.02×10^{-3} K^{-1} and -1.72×10^{-3} K^{-1}.

(Received February 15, 2008; accepted August 14, 2008)

Keywords: Chemical Bath Deposition; Annealing; Four-Point Probe; CdS;

1. Introduction

Cadmium Sulphide (CdS) belongs to II-VI compound semiconductor with direct band gap of about 2.42 eV. In the past years, the deposition and characterization of CdS thin films has a great application potential in the area of electronic and optoelectronic devices fabrications [1-3]. CdS thin films grown on glass substrates using chemical bath deposition method have been extensively studied. There are various methods employed for deposition of CdS thin films such as spray pyrolysis [4-6], pulsed laser deposition [7,8], chemical vapour transport [9,10], vacuum evaporation [11-14], electrodeposition [15-19], sputtering [20,21], successive ionic layer adsorption reaction [22] and chemical bath deposition [23-43]. Among of all methods, the CBD technique has many advantages such as simplicity, no requirement for sophisticated instruments, minimum material wastage, economical way of large area deposition, and no need of handling poisonous gases. The CBD method is a slow process, which facilitates the better orientation of the crystallites with improved grain structure.

In this study, the X-ray diffraction, the energy dispersive X-ray analysis, scanning electron microscopy, four point probe technique, and optical absorption technique are used to characterize the chemically deposited CdS thin films grown on the glass substrates at 60 °C. These films are annealed in air at different temperatures, from 373 K to 773 K in the step of 100 K, to determine the effect of the annealing on the structural, optical and electrical properties. The changes in the optical band gap energy, activation energy, electrical resistivity values depending on the annealing temperature and possible explanations are presented.

2. Experimental details

2.1. Substrate cleaning

The glass slides have been used as the substrate for deposition the films on. The substrate cleaning is very important for this process because of the impurities. Commercially available glass slides (with a size of 75mm x 25mm x 2mm) washed using detergent, chromic acid and deionized water, followed by rinsing in proponal, methanol, and ethanol were used as substrates to deposite the thin films.

2.2. The deposition of the CdS thin films

The CdS thin films have been deposited on the glass substrate using the CBD technique. Aqueous solutions of

1 M cadmium sulphate, 2.25 M hydrazine, 1.4 M thiourea and 25% NH_3 were used to prepare the films. All of the solutions that were used in deposition were clear solutions without precipitation. The glass slides were kept vertically in the beaker. The films were deposited on the glass substrates without stirring at 60 °C for 2 hours. This process was repeated six times to get thicker films and the deposition solution was refreshed for each time. After deposition, the films were washed in distilled water and methanol to remove the loosely adhered CdS particles on the surface and finally dried in air. The as-deposited CdS thin films with 1.2 μm thickness were uniform, well adherent to the substrates and yellow in color.

2.3 Characterization of the CdS thin films

The CdS films were structurally characterized by X-ray powder diffraction, in the range of scanning angle 20-70º with 40 kV at 30 mA, $CuK_{\alpha 1}$ radiation (λ=1.5406 Å) using Phillips diffractometer. The microstructures of these samples were characterized using a LEO scanning electron microscope (SEM) equipped with an energy dispersive X-ray (EDX) spectrometers as well as a computer controlled image analyzer. The optical properties of the CdS films were measured by using UV-Visible spectrophotometer (SHIMADZU UV-1700) at room temperature in the wavelength range 190-1100 nm. The electrical resistivity of the samples was measured by four-point probe technique. The measuring unit was interfaced with a PC for the on-line data acquisition and processing. A Keithley 2400 sourcemeter was used to provide constant current of up to 1 A and the potential drop was detected by a Keithley 2700 multimeter. Platinum wires with diameter of 0.5 mm were employed as current and potential electrodes.

3. Results and discussion

3.1 Structural and morphological studies

The CdS thin films deposited by chemically were annealed in air at different temperatures, 373 K, 473 K, 573 K, 673 K, and 773 K for one hour. The structural properties of these films were investigated by the X-ray diffraction technique. Fig. 1 shows the typical XRD pattern of nanocrystalline CdS films as-deposited and annealed. The diffraction spectra were obtained by scanning 2θ in range 20-70°. The 2θ values of diffraction peaks observed of the CdS films as-deposited are 26.66, 28.15, 44.25, 52.36 and 67.07° ; these correspond to reflections from (111)C,

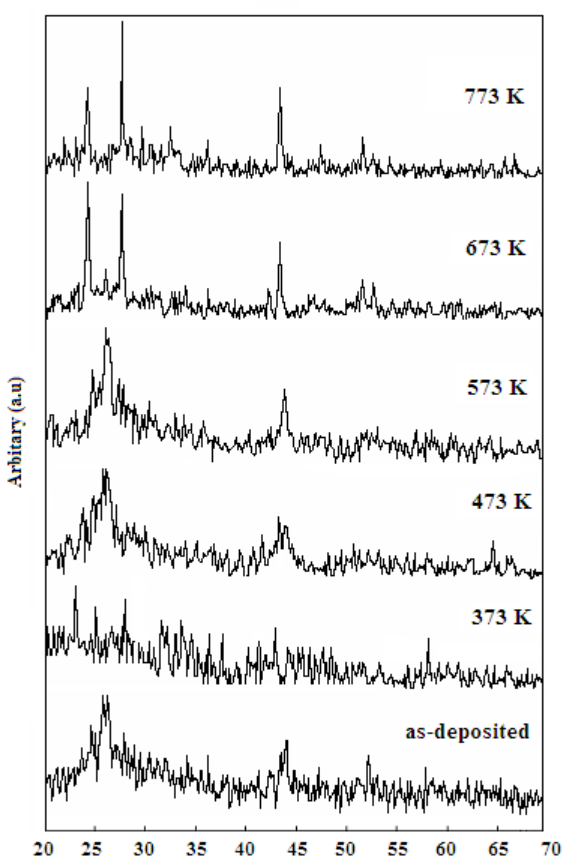

Fig. 1. X-ray diffraction patterns of the CdS films annealed in air atmosphere at different temperatures.

(101)H, (220)C, (311)C, (203)H planes cubic (JPDS card #10-0454) or hexagonal (JPDS card #41-1049) CdS respectively. The diffraction peaks observed are reported as characteristic peaks for CdS thin films by several workers [2, 40, 44, 45]. After annealing at 373 K, the peaks 2θ=43.42 and 2θ=58.66° correspond to the hexagonal (110) and (202), however, the other peaks of CdS do not appear. At 473 and 573 K, the peak at 2θ=26.54° is associated with mixture of hexagonal (002) and cubic (111) planes, the peak at 2θ=44.18° corresponds to the cubic (220) plane, the peak at 2θ=52.42° corresponds to the cubic (311) plane, the peak at 2θ=64.42° corresponds to the cubic (400) plane. The peak at 2θ=58.09° only at 473 K correspond to the cubic (202) plane. The structure of the CdS films exist either the hexagonal (H) or cubic (C). These crystallites are connected to a tissue of polycrystalline structure. Further annealing at 673 K and 773 K, the 2θ values of diffraction peaks observed are 24.78, 26.46, 28.20, 36.52, 43.70, 52.75, 66.82°; these correspond to reflections from (100), (002), (101) (102), (110) (201) (203) planes of hexagonal CdS, respectively. Actually, this is indicated by strong peaks at 2θ=26, 44, and 52°, corresponding to the

(111)C/(002)H, (220)C/(110)H, and (311)C/(201)H phase. With increased annealing temperature, a crystalline restructure occurs in the film in which the hexagonal structure becomes the dominant phase. It was seen that the percentage of hexagonal structured crystallites in the film increases when films are annealed at higher temperatures up to 773 K. Thus, it is more likely that structure of the films is predominantly hexagonal, similar to the other reports [44-47].

The mean size of the crystallites was determined from X-ray diffraction data. We use the standard (111) C reflection at 2θ=26.66º. The Scherer formula,

$$D_{hkl} = \frac{K.\lambda}{\beta Cos\theta} \tag{1}$$

where K is a constant, β is FWHM in radians, λ is the wavelength of X-ray used, θ is the Bragg angle. K value is taken as 0.9 for the calculations. The equation (1) was used for the calculation of the crystallite sizes. The grain sizes of the CdS films increase from 13.6 nm to 49.6 nm with the increasing annealing temperature.

Scanning electron micrographs are helpful in elucidating the incipient growth of the CdS crystals on the glass slides. The SEM micrographs of the as-deposited and the annealed CdS thin films at different temperatures are shown in Fig. 2 (a)-(f). The as-deposited and the annealed at 373 and 473 K films show smooth and uniform surface without cracks or pinholes and well covered to the glass substrate. Small nanosized grains were uniformly distribute over smooth homogenous background. The grains were small with uniform and well-defined grain boundaries. Also, the grains contain irregular needle shape structures which indicate the polycrystalline structure of the samples. The films annealed at 573, 673, and 773 K show some cracks and pinholes. The grains were small with non-uniform shape and well-defined grain boundaries not exist.

The quantitative analysis of the films was carried out by using the EDX technique for the as-deposited film and the annealed films in air atmosphere at different temperatures to study the stoichiometry of the films. Fig. 3 (a)-(f) shows typical EDX patterns with relative analysis. For the as-deposited CdS film the average atomic percentage of Cd:S was 75:29:18.80 showing the sample was slightly cadmium rich. For the annealed films at 373 K, 473 K, 573 K and 673 K the average atomic percentage of Cd was higher than S. The film annealed at 773 K shows that almost all sulfur evaporated which consistent with the results of other works [48]. The result can be clearly seen in Fig. 3 (f).

3.2 Optical properties

The transmissions of the as-deposited and annealed CdS films were measured by UV-Visible spectrophotometer (SHIMADZU UV-1700). All the measurements were made at room temperature.

The thicknesses of the films were calculated from the transmission interference using equation

$$d = \frac{1}{2n\left(\frac{1}{\lambda_2} - \frac{1}{\lambda_1}\right)} \tag{2}$$

where d is the film thickness, n is refractive index, and λ_1 and λ_2 are adjacent maxima or minima of the transmission patterns [49]. Further, the value of the optical band gap energy (E_g) was determined from the absorption spectra of the films by using the following relation [49]:

$$\alpha = A(h\nu - E_g)^n / h\nu \tag{3}$$

where A is a constant, α is absorption coefficient, $h\nu$ is the photon energy and n is a constant, equal to 1/2 for direct band gap semiconductor. The value of the energy where α = 0 is known as energy band gap, E_g. The effect of the annealing on the transmission and α^2 is given in Fig 4. and Fig. 5, respectively. The energy band gap as a function of temperature is shown in Fig. 6. It can be seen in Fig. 5 that the absorption edge of the annealed films has obviously shifted towards longer wavelengths with increasing of the annealing temperature. Also, it is clear to see in Fig. 6 that the energy band gap decreases as the annealing temperature increases. At high temperature (773 K) the film is seen fully degraded in terms of optical absorption at the forbidden region. The scattering of light from the sample was detectable by naked eye only for film annealed at 773 K. This effect reported by other authors as well [42, 50]. So, the value of the energy band gap has not been shown in Fig. 6 at 773 K. As the annealing temperature was increased, the crystallite size of the CdS films was also increased resulting into decrease in band gap. The temperature dependent parameters that affect the band gap are reorganization of the film, sulfur evaporation and self-oxidation of the film. The reorganization of the film, the sulfur evaporation and self-oxidation of the film are affected by the temperature dependent parameters that influence the band gap.

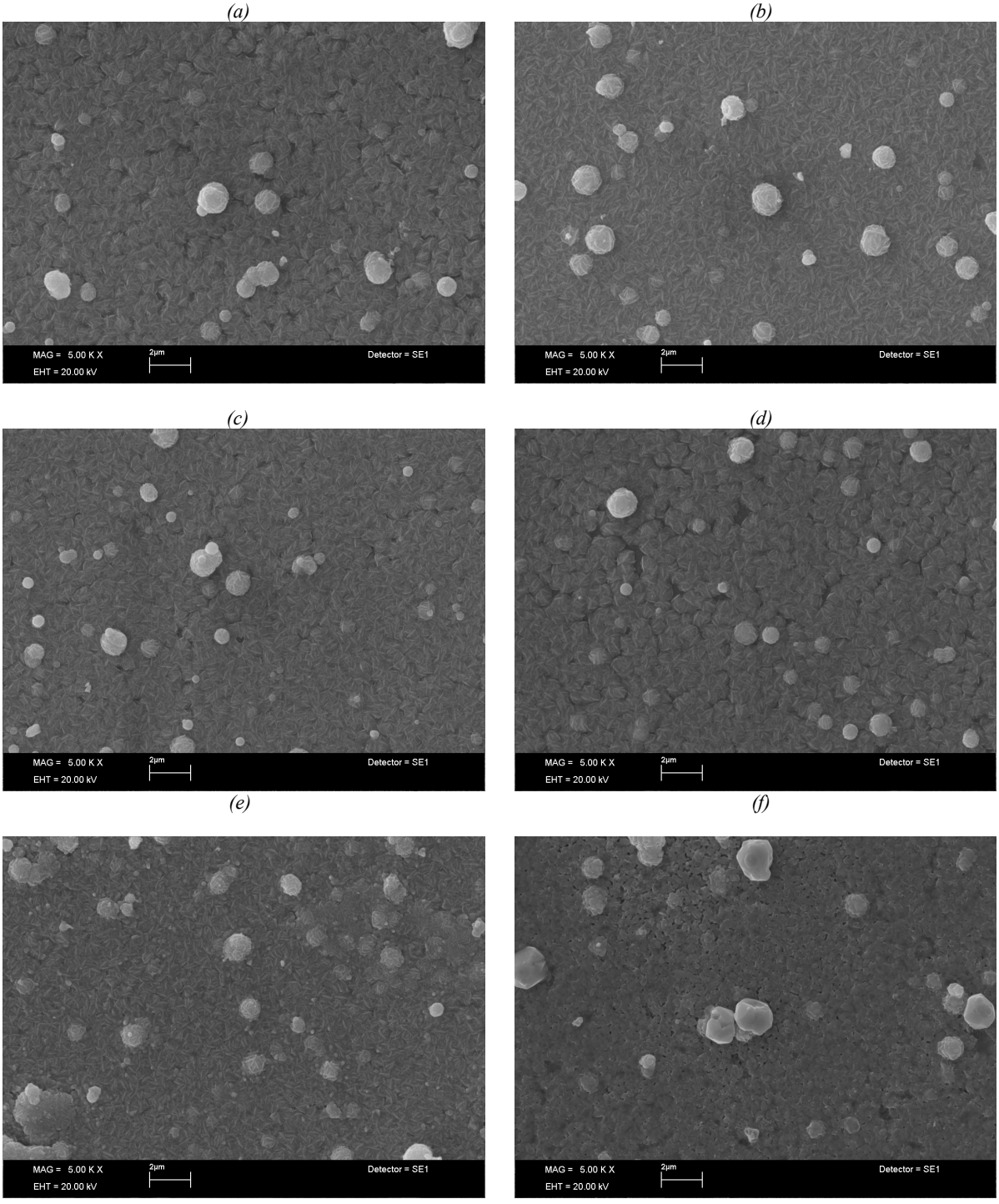

Fig. 2. The SEM micrographs of the films a) as-deposited, and annealed in air atmosphere at b) 373 K c) 473 K d) 573 K e) 673 K and f) 773 K.

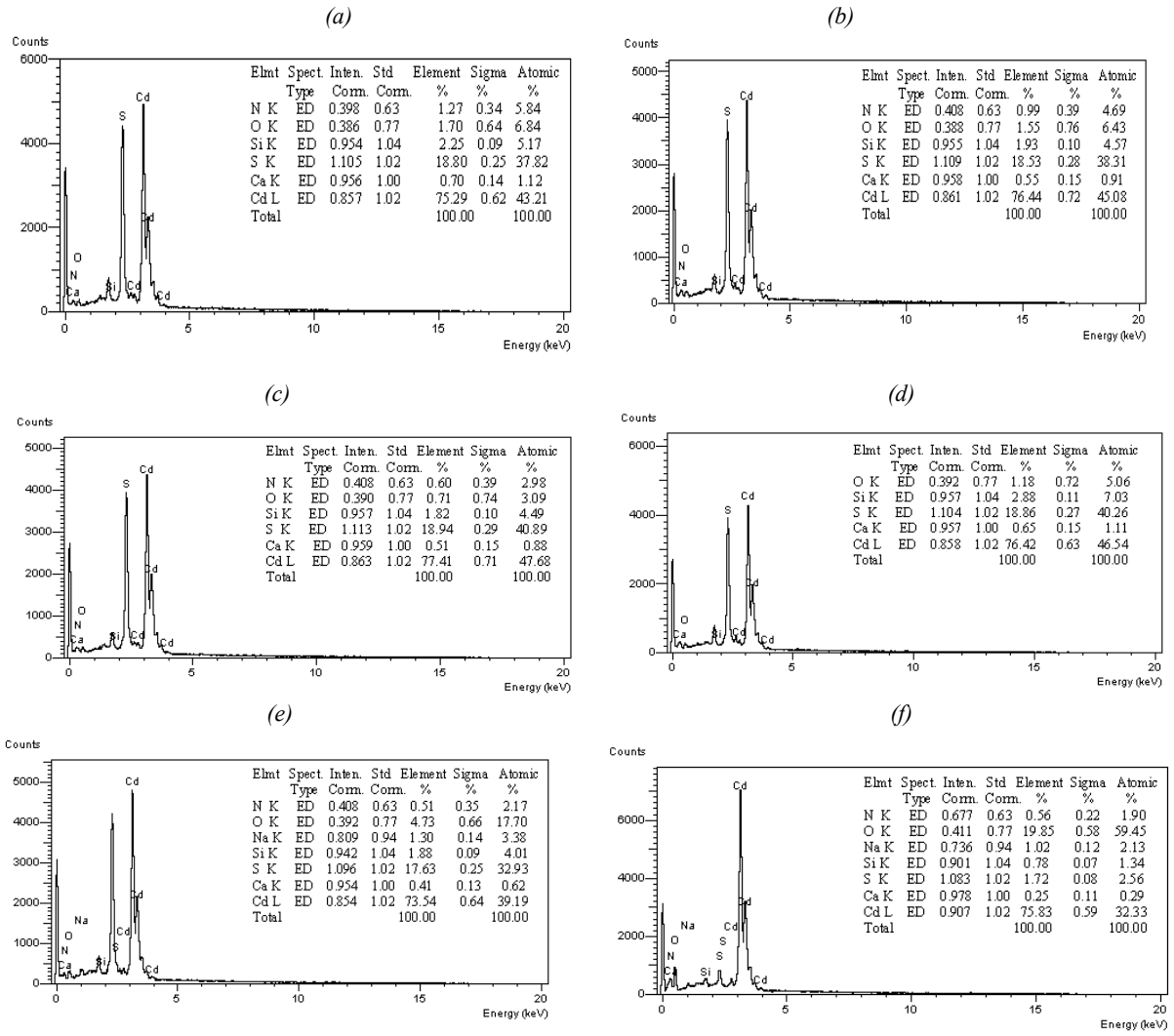

Fig. 3. The EDX analysis of the films a) as-deposited, and annealed in air atmosphere at b) 373 K c) 473 K d) 573 K e) 673 K and f) 773 K.

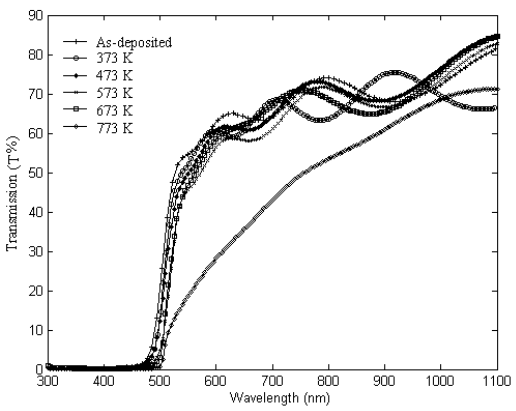

Fig. 4. The transmittance versus wavelength for the as-deposited and the annealed CdS films in air atmosphere at different temperatures.

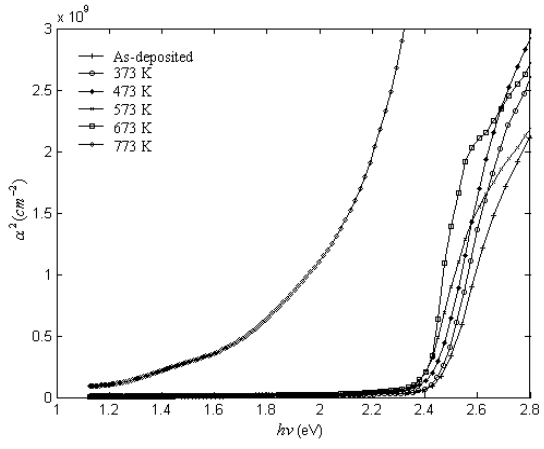

Fig. 5. The α^2 versus $h\nu$ for the as-deposited and the annealed CdS films in air atmosphere at different temperatures.

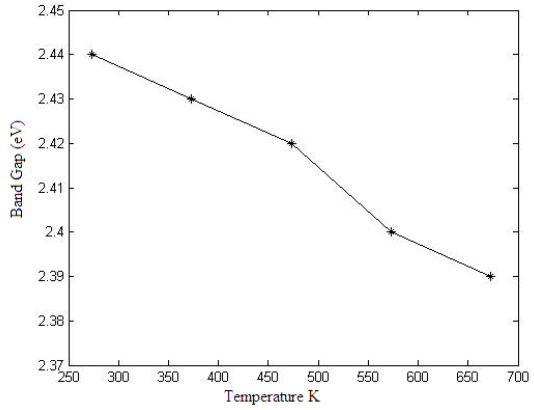

Fig. 6. Plot of the band gap energy of CdS films versus annealing temperature.

3.3 Electrical resistivity and conductivity

The measurements of electrical resistivity and conductivity of the same samples were conducted in the temperature range 300 K– 800 K on rectangular-shape samples with typical 20.0 mm^2, using a standard dc four-point probe method. A four-point probe measurement is performed by making four electrical contacts to a sample surface. [51]. The electrical resistivity, ρ, is determined by loading a direct current, I, through the outer pair of probes and measuring the voltage drop, V, between the inner pair of probes which are positioned at a distance of s = 1 mm, using the following equation:

$$\rho = 2\pi s \frac{V}{I} \tag{4}$$

the errors in the determination of the voltage difference due to the thermoelectric voltage between the electrode and the sample can be eliminated by using a suitable power supply and using the mean of the two measured values in both directions.

The electrical resistivity results of the as-deposited and annealed films were shown in Fig. 7 as a function of temperature. Firstly, it was observed that the resistivity decreases with the increasing the temperature. Thus, the samples show typical semiconductor behaviors. For the as-deposited film, the resistivity values were in order of 10^6 Ω-cm at 305 K and 10^5 Ω-cm at 800 K. The high value of the resistivity of the as-deposited film can be attributed to the dislocations and imperfections of the films. Secondly, the electrical resistivity depends on the annealing temperature. The resistivity decreases with the annealing temperature up to 573 K although it increases at higher annealing temperature. The minimum resistivity was observed in the order of 10^4 Ω-cm for the sample annealed at 473 K.

The activation energy of dark resistivity can be found by using the relation of

$$\rho = \rho_0 \exp(E_a / kT) \tag{5}$$

where ρ is the electrical resistivity at temperature T, ρ_0 is the resistivity at room temperature, k is the Boltzmann constant and E_a is the activation energy. The activation energies of the CdS films were calculated in the range of 0.23 - 0.13 eV in the low temperature region and 0.67 - 0.48 eV in the high temperature region. From Fig. 8, it is observed that the activation energy decreases with the increase in the temperature in high temperature region. However, in low temperature region the activation energy decreases till 573 K then starts to increase.

The temperature coefficient of electrical resistivity (TCR) for the CdS films was also estimated by using the following equation [52],

$$\alpha_{TCR} = (\frac{1}{\rho_1})(\frac{\partial \rho}{\partial T}) = (\frac{1}{\rho_1})(\frac{\Delta \rho}{\Delta T}) \tag{6}$$

where α_{TCR} is the temperature coefficient of electrical resistivity in the temperature between $\Delta T = T_2 - T_1$. $\Delta \rho = \rho_2 - \rho_1$, ρ_1 is the electrical resistivity at T_1 and ρ_2 is the electrical resistivity at T_2. The TCR of the CdS films are calculated in the temperature range 305-800 K, which were found to be between
-2.02x10^{-3} K^{-1} and -1.72x10^{-3} K^{-1}. Materials with a low TCR are used in a wide range of applications such as thermo-electrical devices, flow and temperature sensors in automobiles and resistor in high precision electronic devices [53].

Some typical values of the optical band gap energy, activation energy and temperature coefficient of electrical resistivity for the CdS thin films are given in the Table 1. It is shown that the values of the activation energy obtained from the resistance measurements for the CdS thin films are quite low compared to the values from the optical measurements (Eg/2). The low activation energy values obtained from the resistance measurements gives indication of doped levels (trapped levels or additional energy levels) due to the presence of impurity atoms in the forbidden gap of the semiconducting thin films. Impurities and imperfections drastically affect the electrical properties of a semiconductor [54].

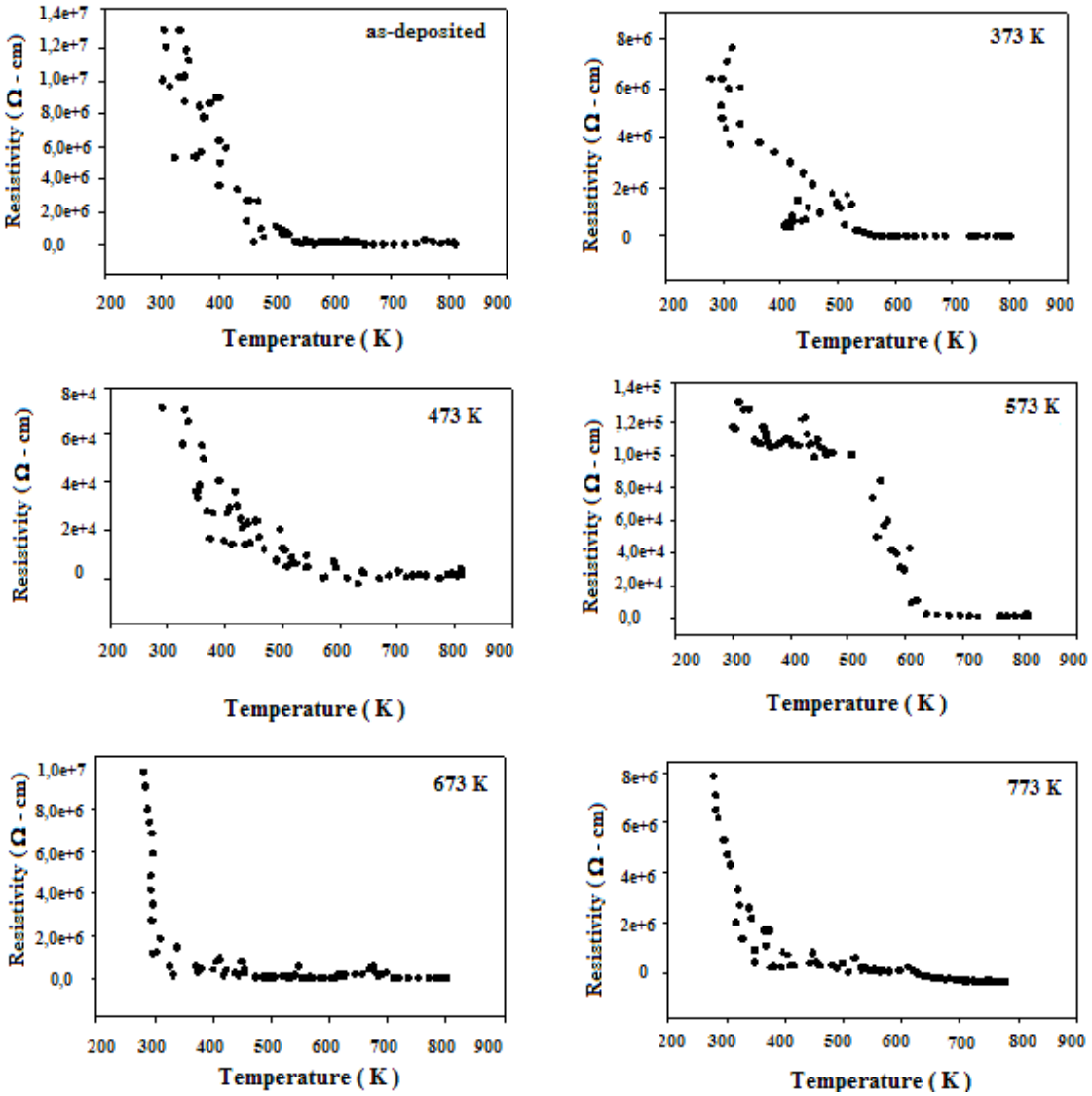

Fig. 7. Temperature dependence of the resistivity of the CdS thin films.

Table 1. The optical band gap, activation energy, and temperature coefficient of electrical resistivity of the as-deposited and annealed CdS thin films.

Annealing temperature (K)	Band gap E_g (eV)	Activation energy (eV)			Temperature coefficient of resistivity α_{TCR} ($\times 10^{-3}$ K^{-1})
		E_a		$E_g/2$	
		LR	HR		305-800
as-deposited	2.43	0.23	0.67	1.22	-1.85
373 K	2.43	0.21	0.64	1.22	-1.72
473 K	2.42	0.17	0.59	1.21	-1.77
573 K	2.40	0.13	0.57	1.20	-1.99
673 K	2.39	0.22	0.50	1.19	-2.02
773 K	1.90	0.23	0.48	0.95	-1.78

R: Low temperature region and HR: High temperature region

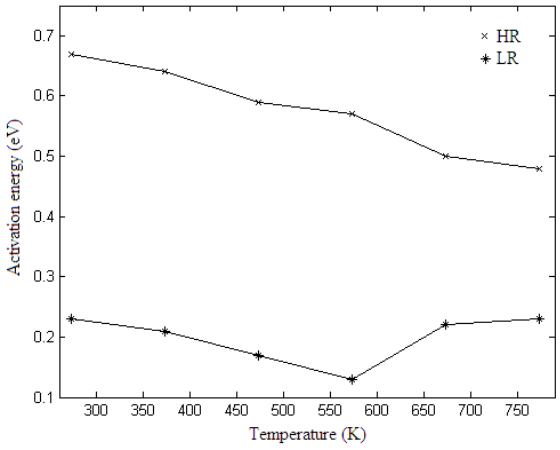

Fig. 8. Plot of the activation energy of CdS films versus annealing temperature.

4. Conclusion

In summary, the influence of annealing in air atmosphere on the optical, structural and electrical properties of the chemically deposited CdS thin films was investigated. We have found out that:

1. The optical energy band gap decreased from 2.43 eV to 2.39 eV with increasing the annealing temperature.

2. The thin films contain nanosized grains which consist of irregular needle shape polycrystalline structure. The sulfur compositions of the films decreased slightly with increasing the annealing temperature in the range of 273 K -673 K and totally evaporated at 773 K which consistent with other studies [48].

3. The activation energies of the CdS films were calculated in the range of 0.23 - 0.13 eV in the low temperature region and 0.67 - 0.48 eV in the high temperature region. Also, these values compared with the values obtained from absorption measurements.

4. The electrical resistivity values of the films decrease with the increasing temperature. And, the temperature coefficients of electrical resistivity have been found to be between -2.02×10^{-5} K^{-1} and -1.72×10^{-3} K^{-1}.

Acknowledgements

This work has been supported in part by Mersin University under contract no. BAP FBE. FB(FS) 2007-2 YL.

References

[1] G. Sasikala, P. Thilakan and C. Subramanian, Sol. Energy Mater. Sol. Cells **62** 275 (2000).
[2] P. Roy and S. K. Srivastava, Materials Chemistry and Physics **95** 235 (2006).
[3] Y.Y. Ma and R.H. Bube, J. Electrochem. Soc. **124** 1430 (1977).
[4] S.J. Castillo, A. Mendoza-Galvan, R. Ramirez-Bon, F.J. Espinoza-Beltran, M. Sotelo-Lerma, J. Gonzalez-Hernandez and G. Martinez, Thin Solid Films **373** 10 (2000).
[5] D.P. Amalnerkar, K. Yamaguchi, T. Kajita and H. Minoura, Solid State Commun. **90** 3 (1994).
[6] Shailaja Kolhe, S.K. Kulkarni, M.G. Takwale and V.G. Bhide, Sol. Energy Mater. **13** 203 (1986).
[7] H.S. Kwork, J.P. Zheng, S. Witanachchi, P. attocks, L. Shi, Q.Y. Ying, X.W. Wang and D.T. Shaw, Appl. Phys. Lett. **52** 1095 (1998).
[8] B. Ullrich, H. Sakai and Y. Segawa, Thin Solid Films **385** 220 (2001).
[9] T.L. Chu, S.S. Chu, C. Ferekides, C.Q. Wu, J. Britt and C. Wang, J. Appl. Phys. **70** 7608 (1991).
[10] R.W. Birkmire, B.E. McCandless and S.S. Hegedus, Sol. Energy **12** 45 (1992).
[11] S.A. Mahmoud, A.A. Ibrahim and A.S. Riad, Thin Solid Films **372** 144 (2000).
[12] S. Mathew, P.S. Mukerjee and K.P. Vijayakumar, Thin Solid Films **254** 278 (1995).
[13] Shailaja Kolhe, S.K. Kulkarni, M.G. Takwale and V.G. Bhide, Sol. Energy Mater. **13** 203 (1986).
[14] U. Pal, R. Silva-Gonzalez, G. Martinez-Montes, M. Gracia-Jimenez, M.A. Vidal and Sh. Torres, Thin Solid Films **305** 345 (1997).
[15] K.L. Choy and B. Su, Thin Solid Films **388** 9 (2001).
[16] G.C. Morris and R. Vanderveen, Sol. Energy Mater. Sol. Cells **27** 305 (1992).
[17] G. Sasikala, R. Dhanasekaran and C. Subramanian, Thin Solid Films **302** 71 (1997).
[18] B. Ullrich, H. Sakai and Y. Segawa, Thin Solid Films **385** 220 (2001).
[19] A.S. Baranski, W.R. Fawcett and A.C. MaDonald, J. Electrochem. Soc. **160** 271 (1984).
[20] L. Martil, N. deDiego and C. Hidalgo, Phys. Stat. Sol. A **94** 587 (1986).
[21] H. Ashour and F. El Akkad, Phys. Status Solidi (a) **184** 175 (2001).
[22] C.D. Lokhande, B.R. Sankapal, H.M. Pathan, M. Muller, M. Giersig and H. Tributsch, Appl. Surf. Sci. **181** 277 (2001).
[23] A. Mondal, T.K. Chaudhuri and P. Pramanik, Sol. Energy Mater. **7** 431 (1983).
[24] H. El Maliki, J.C. Bernede, S. Marsillac, J. Pinel, X. Castel and J. Pouzet, Appl. Surf. Sci. **205** 65 (2003).
[25] S.G. Munde, M.P. Mahabole and R.S. Khairnar, J. Instrum. Soc. India **30** 25 (2000).
[26] P.N. Gibson, M.E. Ozsan, D. Lincot, P. Cowache and D. Summa, Thin Solid Films **361** 34 (2000).
[27] M. Kostoglou, N. Andritsos and A.J. Karabelas, Thin Solid Films **387** 115 (2001).
[28] M.A. Martinez, C. Guillen and J. Herrenro, Appl. Surf. Sci. **140** 182 (1999).
[29] N. Sankar, C. Sanjeeviraja and K.Ramachandran, J. Crystal Growth **243** 117 (2002).

[30] P. O'Brien and T. Saeed, J. Crystal Growth **158** 497 (1996).
[31] R. Lozada-Morales and O. Zelaya-Angel, Thin solids films **281** 386 (1996).
[32] M.T.S. Nair, P.K. Nair, R.A. Zingaro and E.A. Meyers, J. Appl. Phys. **75** 1557 (1994) (3).
[33] T. Hayashi, T. Nishikura, T. Suzuki and Y. Ema, J. Appl. Phys. **64** 3542 (1988) (7).
[34] S.J. Castillo, A. Mendoza-Galvan, R. Ramirez- Bon, F.J. Espinoza-Beltran, M. Sotelo-Lerma, J. Gonzalez-Hernandez and G. Martinez, Thin Solid Films **373** 10 (2000).
[35] D.P. Amalnerkar, K. Yamaguchi, T. Kajita and H. Minoura, Solid State Commun. **90** 3 (1994).
[36] M. Dhanam, R.Balasundraprabhu, S. Jayakumar, P. Gopalakrishnan and M.D. Kannan, Phys. Status Solidi (a) **191** 149 (2002).
[37] M.A. Contreras, M.J. Romero, B. To, F. Hasoon, R. Noufi, S. Ward and K. Ramanathan, Thin Solid Films **403** 204 (2002).
[38] H. Metin and R. Esen, J. Cryst. Growth **258** 141 (2003).
[39] R.S. Mane and C.D. Lokhande, Mater. Chem. Phys. **65** 1 (2000).
[40] I.O. Oladeji, L. Chow, J.R. Liu, W.K. Chu, A.N.P. Bustamante and C. Fredricksen, Thin Solid Films **359** 154 (2000).
[41] A.E. Rakhshani and A.S. Al-Azab, J. Phys., Condens. Matter **12** 8745 (2000).
[42] H. Metin and R. Esen, Semicond. Sci. Technol. **18** 647 (2003).
[43] H. Oumous and H. Hadiri, Thin Solid Films **386** 87 (2001).
[44] S.N. Sharma, R.K. Sharma, K.N. Sood and S. Singh, Mater. Chem. Phy **93** 368 (2005).
[45] S.A. Al Kuhaimi, Vacuum **51** 349 (1998).
[46] E.A. Gluszak and S. Hinckley, Proceedings of the Conference on Optoelectronic and Microelectronic Materials and Devices, Perth, 1998, IEEE Press 426 (1999).
[47] S. Abd-Lefdil, C. Messaoudi, M. Abd-Lefdil and D. Sayan, Phys. Status Solidi (a) **168** 417 1998).
[48] M. Hansen, K. Anderko, Constitutions of Binary Alloys. Newyork: McGraw-Hill Book Company, 303 1958.
[49] J.N. Pankove, Optical Processes in Semiconductors, Dover, New York (1971).
[50] Nair P K, Gomez Daza O, Arias-Carbajal Readigos A, Campos J and Nair M T S, Semicond. Sci. Technol. **16** 651 (2001).
[51] Smits FM. Measurement of sheet resistivities with the four-point probe. The Bell Sys. Tech. J. 711, 1958.
[52] T. Gron et al., Phys. Rev.B **35208** 71 (2005).
[53] C.E. Chi, W.S. Kim, H.H. Hur, Solid State Commun. 120 307 (2001).
[54] R.K. Nkum, A.A. Adimado, H. Totoe, Mater. Sci. Eng. B 35 (1998) 102.

* Corresponding author: hmetin@mersin.edu.tr